Shock-induced interface instability in viscous fluids and metals

Karnig O. Mikaelian

Phys. Rev. E **87**, 031003 — Published 22 March 2013

DOI: 10.1103/PhysRevE.87.031003

Shock-induced interface instability in viscous fluids and metals

Karnig O. Mikaelian

Lawrence Livermore National Laboratory, Livermore, California 94551

We present analytic expressions for the amplitude of perturbations at the interface of two viscous fluids or two metals subjected to a shock. We derive a scaling law by collapsing this 8-parameter problem into 2 (3) non-dimensional variables in the linear (nonlinear) regime. We propose a correspondence principle between viscosity and strength, and a new method for measuring viscosity at high pressure and temperature as an alternative to the "Sakharov method".

PACS numbers 47.20.Bp, 47.20.-k

When a low-density (ρ^l) fluid accelerates a high-density (ρ^h) fluid perturbations $\eta(t)\cos(kx)$ at the interface grow exponentially with time, $\eta(t)\sim e^{\gamma t}$. The growth is much slower in fluids with viscosities μ^l or μ^h: $\gamma_{viscous} << \gamma_{inviscid}$, particularly for short wavelengths $\lambda \equiv 2\pi/k$. Theoretical studies of the viscous Rayleigh-Taylor (RT) instability [1,2] have found applications in geophysical experiments [3,4] and break-up of viscous bubbles [5,6]. Similarly, plasticity of metals characterized by a yield strength Y is an obvious stabilizing property: Metals don't flow unless subjected to a large pressure $>> Y$ and even then the subsequent growth is much slower than in ordinary fluids. Given Y and/or shear modulus G of a metal there is a critical amplitude η_0^c and wavelength λ^c

below which perturbations will not grow [7, 8, 9]. Both cut-offs are inversely proportional to the acceleration g. Away from these cut-offs there is a fastest growing mode, similar to the viscous case, studied in detail by Terrones who extended earlier single-material studies to two materials but did not include plastic flow [10]. Barnes *et al.* performed RT experiments on Aluminum driven by high explosives at ~100 kb [11], and recent experiments use lasers to extend the same technique (suppression of RT growth as a measure of strength) to ~5 Mb [12].

One expects a similar suppression of the Richtmyer-Meshkov (RM) instability in viscous fluids or metals when the system is subjected to a shock, instead of a constant acceleration, inducing a jump velocity Δv (positive, in our convention, if passing from light to heavy, negative otherwise). Much less work has been done in this area. Three different expressions have been given for viscous RM [13, 14, 15]. We compare them and present a fourth one. Many of the break-up experiments start with a shock [6]. It is common to use the "Sakharov method", viscous damping of a perturbed shock front, to measure viscosity at high pressure and temperature [16]. We propose an alternative method: Viscous damping of a perturbed interface. Its earlier proposed counterpart in metals [17] has been successfully carried out in recent experiments [18, 19]. Drucker mentions a comparison between viscosity and strength [8]. Several strength experiments are analyzed in terms of viscosity [12, 20]. We provide an approximate relationship between μ and Y. Combining it with viscous results leads to asymptotic expressions in the linear ($\eta k << 1$) as well as the nonlinear ($\eta k >> 1$) regimes, in agreement with models and simulations of plastic RM growth [18, 21].

We address questions of scaling: What are the parameters that affect the growth factor $\eta(t)/\eta(0)$? This is an 8-parameter problem: $\eta_0 \equiv \eta(0)$, k, ρ^h, ρ^l, μ^h, μ^l (or Y^h, Y^l), $\Delta\mathrm{v}$, t. We present an explicit expression for $\eta(t)$ finding that the problem collapses into two or three variables only: an appropriately defined Reynolds number and a non-dimensional time. The third variable, needed only in the nonlinear regime, is $\eta_0 k$. We answer questions such as: Does the growth depend on the product, sum, or some other combination of μ^h and μ^l? *Ditto* for Y.

Viscosity. Based on approximate eigenvalues, the first linear treatment of the viscous RM instability gave [13]

$$\eta(t) = \eta_0 + \dot{\eta}_0(1 - e^{-2\nu k^2 t})/2\nu k^2 \tag{1}$$

where $\dot{\eta}_0 = \eta_0 \Delta\mathrm{v} k A$ is the inviscid growth rate with $A \equiv (\rho^h - \rho^l)/(\rho^h + \rho^l)$, $\nu \equiv (\mu^h + \mu^l)/(\rho^h + \rho^l)$. Eq. (1) asymptotes to

$$\eta_\infty = \eta_0 + \dot{\eta}_0 / 2\nu k^2 = \eta_0(1 + \Delta\mathrm{v} A / 2\nu k). \tag{2}$$

Subsequently, an alternative expression was presented [15]:

$$\eta(t) = \eta_0 + \dot{\eta}_0 t(1 - Ct^{1/2}) \tag{3}$$

with $C \equiv 16k\sqrt{\mu^h \mu^l \rho^h \rho^l} / [3\sqrt{\pi}(\sqrt{\mu^h \rho^h} + \sqrt{\mu^l \rho^l})(\rho^h + \rho^l)]$. This must not be used when $\rho^h = 0$ or $\rho^l = 0$, or when $\mu^h = 0$ or $\mu^l = 0$ because C depends on their *product*. In contrast, ν in Eq. (1) depends on the *sum* and therefore viscous effects persist as long as $\mu^h + \mu^l \neq 0$.

Eq. (3) has another limitation: It can apply for "early" times only. It may be used, if at all, only for $t < 4/9C^2$ because it gives $d\eta/dt = 0$ at $t = 4/9C^2$ and becomes negative(!) for $t > 4/9C^2$, clearly unphysical.

Despite these shortcomings we found a few cases where Eq. (3) did better than Eq. (1) at early times. Our procedure was to compare Eq. (1), Eq. (3), and full Navier-Stokes solutions with the hydrocode CALE [22]. At present CALE can treat only constant viscosities but this was enough for our purpose. These simulations confirmed the above statements: Viscous effects persist even when only one of the fluids has viscosity, the controlling parameter is ν, and $\dot{\eta}$ does not reverse sign at any time. But there were also cases, mostly with $\mu^h \sim \mu^l$, where Eq. (3) did better than Eq. (1) at early times.

Our first attempt to improve upon Eq. (1) was to use exact eigenvalues. In general, when one of them vanishes (say $\gamma_+ = 0$) the result is

$$\eta(t) = \eta_0 - \dot{\eta}_0(1 - e^{\gamma_- t})/\gamma_- . \tag{4}$$

In the approximation of [13] $\gamma_- = -2\nu k^2$, hence Eq. (1). Using exact eigenvalues we find that $\gamma_+ = 0$ still, but γ_- is different. To our surprise, however, using exact eigenvalues gave substantially *worse* results. For example, for the simplest, one-fluid case we find $\gamma_- = -2[4 + (\sqrt{297} - 17)^{1/3} - (\sqrt{297} + 17)^{1/3}]\nu k^2/3 \approx -0.9126\nu k^2$. In fact the equation $\eta(t) = \eta_0 + \dot{\eta}_0(1 - e^{-0.9126\nu k^2 t})/0.9126\nu k^2$ can be found in the summary by Bakhrakh *et al.* [14]. Its asymptotic growth is more than twice larger and completely ruled out by our numerical simulations.

The only remaining option is to treat the problem as an initial-value problem, similar to the viscous RT instability [23]. This approach is substantially more complex and to date there are no exact results for arbitrary $\mu^{h,l}$. We have succeeded, however, in deriving an exact and general expression for the asymptote η_∞ and *the result is Eq. (2)*. As for $\eta(t)$, the general Laplacian which must be inverted is too complicated to carry out analytically. We found, however, the following expression extremely accurate in describing our CALE results:

$$\eta(t) = \eta_0 + \frac{\dot{\eta}_0}{4\nu k^2} erfc(-\sqrt{\tau}) + \frac{\dot{\eta}_0}{\nu k^2} \sum_{i=2}^{4} \frac{Z_i}{D'(Z_i)} e^{(Z_i^2-1)\tau} erfc(-Z_i\sqrt{\tau}) \qquad (5)$$

where $erfc(z)$ is the complimentary error function $1-err(z)$, $\tau \equiv \nu k^2 t$, $Z_2 = 1/4$, $Z_{3,4} = (-7 \pm 4i\sqrt{11})/9$, $D'(Z_2) = -155/64$, and $D'(Z_{3,4}) = 8(1111 \mp 28i\sqrt{11})/729$. Together with $Z_1 = 1$, $D'(1) = 4$, they satisfy the four sum rules $\sum_{i=1}^{4} 1/D'(Z_i) = \sum_{i=1}^{4} Z_i/D'(Z_i) = \sum_{i=1}^{4} Z_i^2/D'(Z_i) = \sum_{i=1}^{4} Z_i^3/D'(Z_i) - 1 = 0$.

Eq. (5) has several surprising properties: the Atwood number A does not appear in it except for $\dot{\eta}_0 = \eta_0 \Delta v k A$. It is an exact expression only if $\nu^h = \nu^l$ ($\nu^{h,l} \equiv \mu^{h,l}/\rho^{h,l}$), but it is also an extremely good approximation for arbitrary $\nu^{h,l}$. Its asymptote, η_∞, agrees with Eq. (2), the only exact formula for arbitrary $\nu^{h,l}$. What is surprising is that there are actually infinitely many solutions, each associated with a different A and all giving approximately the *same* result, within a few percent, which is the reason why A does not appear in Eq. (5). In the exact solution for $\nu^h = \nu^l$ the 6 constants Z_i and $D'(Z_i)$, $i = 2,3,4$ are determined from $Z^3 + (2-A^2)Z^2 + (1+2A^2)Z - A^2 = 0$ and $D'(Z) = 4Z^3 + 3(1-A^2)Z^2 + 2(3A^2-1)Z - 1 - 3A^2$. The solution we chose corresponds to $A = 5/6$ because it gives particularly simple expressions.

We illustrate with an example: $\rho^h = 4\,\text{g/cm}^3$, $\rho^l = 1\ \text{g/cm}^3$, $\Delta\text{v} = 0.1\,\text{cm/ms}$, $\lambda = 2.5$ cm, $\eta_0 = 30\,\mu\text{m}$, $\mu^h = 0.32\,\text{Pa-s}$, and $\mu^l = 2\mu^h$. Fig. 1 shows $\eta(t)$ as calculated by Eqs. (1), (3), (5), and CALE. Eq. (1) overestimates $\eta(t)$ at early times but its asymptote, Eq. (2), is reproduced by Eq. (5) and by CALE. Eq. (3) shows better agreement with CALE but only at early times – its behavior after 89 ms ($4/9C^2$) is unphysical. Only Eq. (5) agrees with CALE both at early and late times. The reader should be surprised at this because Eq. (5) is exact only for $\nu^l = \nu^h$ and $A = 5/6$ while in this example $\nu^l = 8\nu^h$ and $A = 3/5$. We repeat that other Z_i solutions give essentially the same $\eta(t)$ when substituted in Eq. (5).

Eq. (5) displays simple scaling: Out of the eight independent variables only two combinations are relevant: $\Delta\text{vA}/\nu\text{k}$ and $\nu\text{k}^2 t$. It is customary to define a Reynolds number as a ratio of inertial to viscous forces. We propose $\text{Re} = |\Delta\text{v}|\text{A}/\nu\text{k}$ so that $\eta(t)/\eta_0 = f(\pm\text{Re},\tau)$. Eq. (2) reads $\eta_\infty = \eta_0(1 \pm \text{Re}/2)$. Note that $\eta_\infty = 3\eta_0$ or $-\eta_0$ when $\text{Re} = 4$, a case discussed below.

Strength. We now consider shocks in ideal elastic-plastic solids characterized by a constant shear modulus G and yield strength Y. Early work, primarily experimental, is summarized in [14]. Here we follow-up on the suggestion that strength may be treated as viscosity because they found that using a $\mu - Y$ relationship in our analytic viscous formulae gave reasonable results for RT strength experiments [20]. There are strength effects which cannot be duplicated by viscosity such as the Drucker and Miles cut-offs η_0^c and λ^c [24]. Since both are proportional to $1/g$ they vanish in the RM case where $g \to \infty, \int g dt = \Delta\text{v}$, yielding $\dot{\eta}_0 = \eta_0 \Delta\text{v} k A$ as in the fluid case.

We find that no $\mu - Y$ relationship can provide exact agreement between η^Y and η^μ – only a qualitative agreement can be obtained, within 30-40%, made possible by two opposing trends: η^Y grows faster but saturates earlier, while η^μ grows slower but saturates later. The following relationship

$$Y \approx 2|\dot{\eta}_0|k\mu/3 \tag{6}$$

provides that qualitative agreement. Eq. (6) means that η between two fluids of viscosities $\mu^{h,l}$ will evolve similar to the case of two metals whose yield strengths $Y^{h,l}$ satisfy Eq. (6). Actually, only the sum $Y^h + Y^l$ is important. We have verified this by direct numerical simulations.

A comparison between η^μ (in black) and η^Y (in red) is given in Fig. 2. The lower curves refer to the same problem as in Fig. 1, so the same CALE curve is reproduced in black. In red is the problem with strength where $Y^{h,l}$ are related to $\mu^{h,l}$ by Eq. (6): $Y^h = 0.24Pa$, $Y^l = 2Y^h = 0.48Pa$. The shear moduli are taken to be 10^3 times larger – they control mostly the oscillations after η^Y reaches its maximum [14, 21]. The two upper curves in Fig. 2 refer to the same problem but with the shock generated in the heavy fluid inducing the same $|\Delta \mathrm{v}|$, now taking $\mu^l = 0$. There is growth after the phase reversal ($\Delta \mathrm{v}$ and hence $\dot{\eta}_0$ are negative), and a reshock occurs at 270 ms, just as η^μ and η^Y cross. The inset shows the two interfaces at this time; they have the same amplitude but the shape of the Y–problem is triangular. This difference in shape persists after reshock but the amplitudes continue to track each other.

Needless to say, Eq. (6) does *not* mean that strength depends on η_0, Δv, k, etc.! It is only a correspondence principle to convert μ–derived results to Y. Substituting it in Eq. (2) one obtains

$$\eta_\infty = \eta_0 + \dot{\eta}_0 |\dot{\eta}_0| (\rho^h + \rho^l) / 3k(Y^h + Y^l) \tag{7}$$

to be compared with $\eta_0 + 0.29\rho\dot{\eta}_0^2 / kY$ for a single fluid [21]. Let us apply Eq. (7) to the case $\eta_\infty = -\eta_0$, i.e. the perturbation stops growing after a complete phase change. For strength, the requirement in a single fluid is

$$Y_{\eta_\infty = -\eta_0} = \eta_0 (\Delta\text{v})^2 k\rho / 6\,. \tag{8}$$

As shown in Fig. 12 of [17], this happens for the SG model in Aluminum. Using $\rho = 2.7$ g/cm^3, $\eta_0 = 0.02$ cm, $\lambda = 1$ cm, $\Delta\text{v} = 3.5/15 = 0.23$ cm/μs (all taken from [17]), the rhs of Eq. (8) gives $3\,\text{kb}$, agreeing with the Y_0 ($2.9\,\text{kb}$) of SG. This after-the-fact comparison builds confidence that Eq. (6) is a reasonable relationship. Eq. (6) appears to work for the RT case also when we replace the inverse time scale $|\dot{\eta}_0| k$ by $\sqrt{gkA}$, as long as the amplitude and wavelengths are above the cut-offs. A similar relation was proposed by Colvin *et al*. with the strain-rate serving as the inverse time scale calculated from experimental conditions or numerical simulations [20].

Compressibility. The theory and simulations discussed so far have been limited to incompressible fluids – we used ideal equations-of-state with high adiabatic indices so the densities change very little. By running highly compressible problems and comparing with Eq. (5) we found that using the post-shock viscosity ν_{after} is a reasonable way of accounting for compressibility, the same way that Richtmyer and Meyer and Blewett prescribed using the post-shock Atwood number A_{after} [25]. Note that since $\nu \sim \mu / \rho$ and $\rho_{after} > \rho_{before}$, compressibility decreases ν and therefore increases the growth when $\mu = const$. The same effect will arise when shocks heat the fluids and, in general, reduce their viscosities.

As an example, we ran a compressible CALE problem setting adiabatic indices equal to 5/3. The postshock densities increased 1.6 times and the growth factor GF was 23.3. Using $\nu_{preshock}$, Eq. (5) predicted too small a GF: 18.8. Using $\nu_{postshock}$, which of course is 1.6 times smaller than $\nu_{preshock}$, gave GF=23.5 in good agreement with CALE.

The only method proposed so far to measure viscosities at high pressures and temperatures is the "Sakharov method" reviewed extensively in [16]: Measure the decay of a corrugated shock in a viscous fluid. We believe the viscous RM instability is a more effective way because $\eta_\infty \propto 1/\nu$ from Eq. (2). The growth depends on the sum of the viscosities on either side of the interface, but choosing one of the fluids to be inviscid isolates the viscosity of the other. We have verified, by numerical simulations, that the method proposed for strength [17] works equally well with viscosity.

Nonlinearity. Layzer's nonlinear model for a single inviscid fluid [26] and its extension to two fluids [27] are natural candidates for a nonlinear viscous model – keep the viscous term in the Bernoulli equation. This was done by Sohn [28]. However, we find that this model is even more limited than the inviscid model, the limitations and failures of which were reported in [29].

(We should point out that in the linear limit this viscous model reduces to our model and that Sohn's linear RM solution (Eq. (11) in [28]) is in error - the correct $\eta(t)$ was given in [13], reproduced here as Eq. (1)).

We find that the model gives reasonable results only for the bubble and only for $A = 1$. If $A \neq 1$ the model predicts "negative viscosity" for large initial amplitudes. Thus we concentrate on the original single-fluid Layzer model augmented by viscosity:

$$(2\eta_2 + ck/2)(\ddot{\eta} + 2\nu k^2\dot{\eta}) + c^2k^2\dot{\eta}^2/4 + 2g\eta_2 = 0, \tag{9}$$

where $\eta_2(t) = -ck\{1 + [(1+c)\eta_0 k - 1]e^{-k(1+c)(\eta-\eta_0)}\}/4(1+c)$ and $c = 1(2)$ for 3D(2D), as in the inviscid case [29].

Eq. (9) can be solved analytically by the (η^*, t^*) technique: Use the linear solution until $\eta = \eta^* \equiv 1/(1+c)k$ followed by the nonlinear solution (given below) which can be easily obtained since η_2 becomes constant for $\eta_0 = \eta^*$ [29]. Setting $g = 0$ (this is not necessary – we will consider the RT problem elsewhere) we find

$$\eta(t) = \eta_0 + [2/(k+ck)]\ln[1 + (1+c)(\dot{\eta}_0/4\nu k)(1 - e^{-2\nu k^2 t})] \tag{10}$$

confirming again that "the nonlinear solution is essentially the logarithm of the linear solution" – compare with Eq. (1).

From Eq. (10) the nonlinear asymptote is

$$\eta_\infty = \eta_0 + [2/(k+ck)]\ln[1 + (1+c)\dot{\eta}_0/4\nu k] \tag{11}$$

to be compared with Eq. (2). Combining this with Eq. (6) we obtain

$$\eta_\infty = \eta_0 + [2/(k+ck)]\ln[1 + (1+c)\dot{\eta}_0^2\rho/6Y]. \tag{12}$$

Setting $c = 2$ this equation agrees quite well with the asymptotic 2D bubble amplitudes computed by Dimonte *et al*. (Fig. 2 in Ref. [18]).

How about the spike? Zhang [30] proposed using the Layzer model with $\eta < 0$ for spikes, and indeed this works for the inviscid spike when $A = 1$ [29]. However, we find that the viscous model is a poorer representation of the spike when we solve Eq. (9) numerically with $\eta_0 < 0$.

Fig. 3 illustrates the above observations. The problem is the same as the He/Xe problem used previously for its large Atwood number, $A \approx 0.94$, adding viscosity (black curves) or strength (red curves) to the heavy "Xe", using Eq. (6) for the $\mu - Y$ correspondence. These 4 curves, calculated by 2D CALE, are compared with the numerical solution of Eq. (9) for the spike and with the analytic solution, Eq. (10), for the bubble. The initial amplitude is 0.7 cm and $\lambda = 13$ cm, so $\eta_0 \approx \eta^* = 1/3k$, and $\Delta \mathrm{v} = 8.25$ cm/ms. For viscosity we chose $\mu = 0.2$ Pa-s giving $\mathrm{Re} = 45$. From Eq. (6) the corresponding Y is ≈ 160 Pa. The inset shows the interfaces as calculated by CALE at $t = 6$ ms when they have moved 50 cm. The $\mu - Y$ correspondence does better for the bubble than for the spike in the nonlinear regime (there is no bubble/spike difference in the linear regime). Eq. (10) is a good model for the bubble, but the spike is overestimated. This may be due to 1) $A = 1$ vs. 0.94, 2) We have used ν_{after}, and 3) Nonlinear effects suppress $\dot{\eta}_0$ [19].

Conclusions. The viscous RM instability in the linear and incompressible regime is well described by Eq. (5) and, to a lesser degree, by the much simpler Eq. (1). Eq. (2) is exact. The $\mu - Y$ surrogacy is approximate and based on similarity of $\eta^{\mu}(t)$ and $\eta^{Y}(t)$ when μ and Y satisfy Eq. (6).

Generally, we find μ to have a weaker effect in nonlinear problems, which can be understood by comparing Eqs. (2) and (11): $\eta_\infty \sim 1/\nu$ in the linear regime, but $\sim \ln(1/\nu)$ in the nonlinear regime. Similarly for Y. RM experiments with viscosity, as an alternative to the "Sakharov method", will be more discriminating with small η_0. We hope our findings will spur further experimentation.

This work was performed under the auspices of the U. S. Department of Energy by Lawrence Livermore National Laboratory under Contract DE-AC52-07NA27344.

REFERENCES

[1] R. Bellman and R. H. Pennington, Q. Appl. Math. **12**, 151 (1954).

[2] S. Chandrasekhar, *Hydrodynamic and Hydromagnetic Stability* (Oxford University Press, London, 1968).

[3] P. Olson and C. Kincaid, J. Geophys. Res. **96**, 4347 (1991).

[4] W. S. D. Wilcock and J. A. Whitehead, J. Geophys. Res. **96**, 12193 (1996).

[5] D. D. Joseph, G. S. Beavers, and T. Funada, J. Fl. Mech. **453**, 109 (2002).

[6] T. G. Theofanous, Ann. Rev. Fl. Mech. **43**, 661 (2011).

[7] J. Miles, GAMD-7335, General dynamics (1966) (unpublished).

[8] D. C. Drucker, Ing. Arch. **49**, 361 (1980).

[9] J. W. Swegle and A. C. Robinson, J. App. Phys. **66**, 2838 (1989); A. C. Robinson and J. W. Swegle, ibid. **66**, 2859 (1989).

[10] G. Terrones, Phys. Rev. E **71**, 036306 (2005).

[11] J. F. Barnes *et al*., J. App. Phys. **45**, 727 (1974) and *ibid.* **51**, 4678 (1980).

[12] H.-S. Park *et al.*, Phys. Rev. Lett. **104**, 135504 (2010).

[13] K. O. Mikaelian, Phys. Rev. E **47**, 375 (1993).

[14] S. M. Bakhrakh *et al*., UCRL-CR-126710 (1997) (unpublished).

[15] P. Carlès and S. Popinet, European J. Mech. B Fluids **21**, 511 (2002).

[16] G. H. Miller and T. J. Ahrens, Rev. Mod. Phys. **63**, 919 (1991).

[17] K. O. Mikaelian, Phys. Fl. **17**, 034101 (2005).

[18] G. Dimonte *et al*., Phys. Rev. Lett. **107**, 264502 (2011).

[19] W. T. Buttler *et al*, J. Fl. Mech. (*in press*).

[20] J. D. Colvin *et al.*, J. Appl. Phys. **93**, 5287 (2003).

[21] A. R. Piriz *et al*., Phys. Rev. E **78**, 056401 (2008).

[22] R. E. Tipton, CALE Users Manual (unpublished) and in *Megagauss Technology and Pulsed Power Applications*, edited by C. M. Fowler, R. S. Caird, and D. J. Erickson (Plenum, New York, 1987), p. 299. R. T. Barton, in *Numerical Astrophysics*, edited by J. M. Centrella, J. M. LeBlanc, and R. L. Bowers (Jones and Bartlett, Boston, 1985), p. 482.

[23] A. Prosperetti, Phys. Fl. **24**, 1217 (1981).

[24] A. R. Piriz *et al*., Phys. Rev. Lett. **105**, 179601 (2010); H.-S. Park *et al*., *ibid.* **105**, 179602 (2010).

[25] K. A. Meyer and P. J. Blewett, Phys. Fl. **15**, 753 (1972).

[26] D. Layzer, Astrophys. J. **122**, 1 (1955).

[27] V. N. Goncharov, Phys. Rev. Lett. **88**, 134502 (2002).

[28] S.-I. Sohn, Phys. Rev. E **80**, 055302 (2009).

[29] K. O. Mikaelian, Phys. Rev. E **78**, 015303 (2008).

[30] Q. Zhang, Phys. Rev. Lett. **81**, 3391 (1998).

Figure Captions

Fig. 1. Comparison of Eqs. (1), (3), and (5) with a CALE simulation of the problem discussed in the text.

Fig. 2. Four growth factors calculated by CALE: black for μ and red for Y. The lower curves refer to the same problem as in Fig. 1 and have $\mathrm{Re} \approx 13$. The upper curves refer to a problem with $\Delta\mathrm{v}$ replaced by $-\Delta\mathrm{v}$ (shock generated in the heavy fluid) and $\mu^l = 0$, hence $\mathrm{Re} \approx 38$. Reshock occurs at 270 ms. The inset shows the interfaces for the μ and Y problems at 270 ms, the vertical scale greatly enhanced for clarity. In both problems $Y^{h,l}$ and $\mu^{h,l}$ are related by Eq. (6).

Fig. 3. CALE calculation of bubbles (lower curves) and spikes (upper curves) for the $A \approx 1$ problem discussed in the text, black referring to μ and red to Y, related by Eq. (6). Blue dashed lines are from Eq. (9) solved numerically with $\eta_0 = -0.7\,\mathrm{cm}$ for the spike, and from Eq. (10) for the bubble. The inset shows the interfaces for the μ and Y problems at $6\,\mathrm{ms}$. $\mathrm{Re} = 45$.

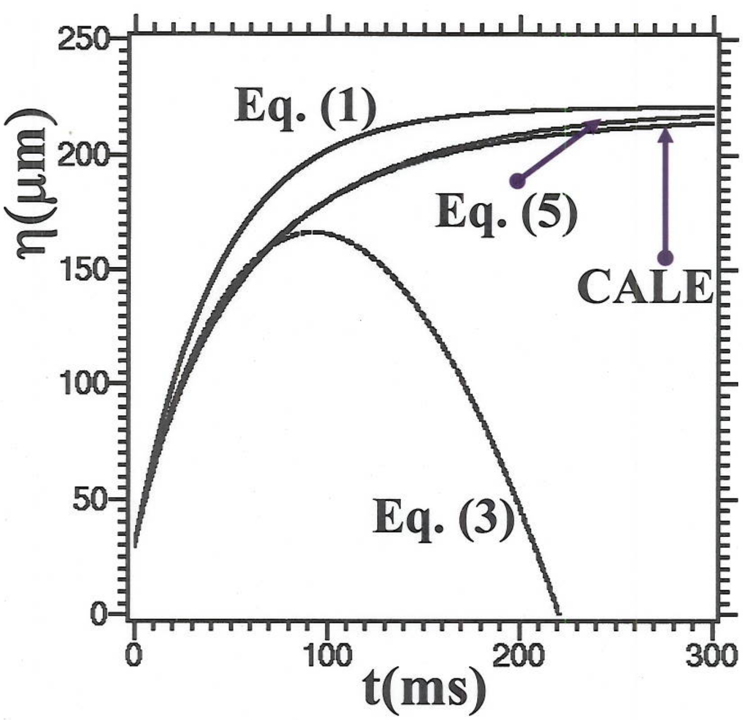

Fig. 1

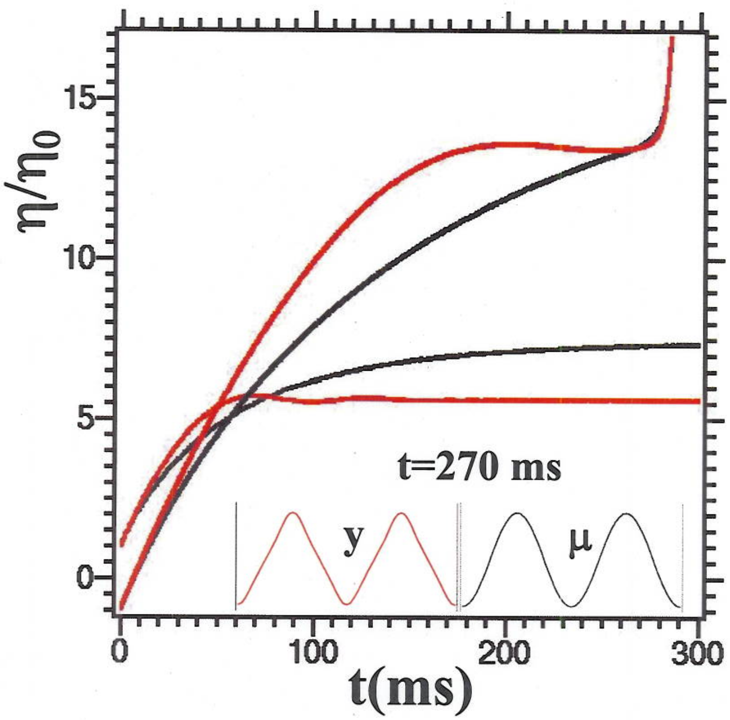

Fig. 2

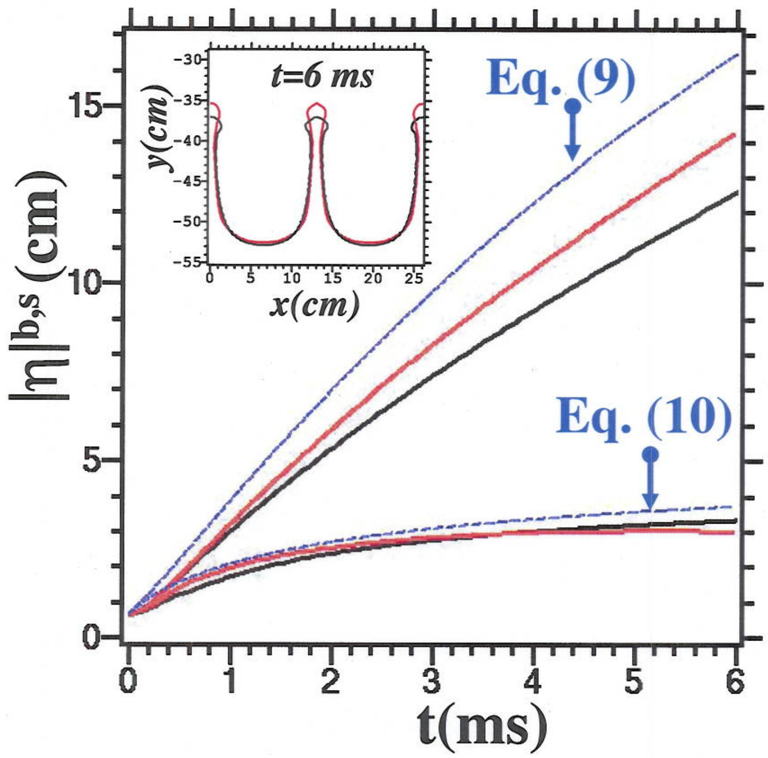

Fig. 3